0026-895X/98/040750-09$3.00/0

MOLECULAR PHARMACOLOGY, **53:**750–758 (1998).

Identification and Characterization of Two Cysteinyl-Leukotriene High Affinity Binding Sites with Receptor Characteristics in Human Lung Parenchyma

VALÉRIE CAPRA, SIMONETTA NICOSIA, DANIELA RAGNINI, MAURIZIO MEZZETTI, DIETRICH KEPPLER, and G. ENRICO ROVATI

Laboratory of Molecular Pharmacology (V.C., S.N., D.R., G.E.R.), Institute of Pharmacological Sciences, University of Milan, 20133 Milan, Italy, IRCCS European Institute of Oncology (M.M.), Department of Thoracic Surgery, Milan, Italy, and Deutsches Krebsforschungszentrum (D.K.), Division of Tumor Biochemistry, Heidelberg, Germany

Received October 30, 1997; Accepted December 5, 1997

This paper is available online at http://www.molpharm.org

ABSTRACT

We report the characterization of two distinct binding sites with receptor characteristics for leukotriene (LT)D_4 and LTC_4 in membranes from human lung parenchyma. The use of *S*-decyl-glutathione allowed us to characterize a previously unidentified high affinity binding site for LTC_4. Computerized analysis of binding data revealed that each leukotriene interacts with two distinct classes of binding sites (K_d = 0.015 and 105 nM for LTC_4 and 0.023 and 230 nM for LTD_4) and that despite cross-reactivity, the two high affinity sites are different entities. LTD_4 binding sites displayed features of G protein-coupled receptors, whereas LTC_4 binding sites did not show any significant modulation by guanosine-5′-(β,γ-imido)triphosphate or stimulation of GTPase activity. The antagonists ICI 198,615 and SKF 104353 were unselective for the high and low affinity states of LTD_4 receptor, whereas only SKF 104353 was able to recognize the two [^{3}H]LTC_4 binding sites although with different affinities. These data indicate that in human lung parenchyma, LTD_4 and LTC_4 recognize two different binding sites; these binding sites are different entities; and for LTD_4, the two binding sites represent the interconvertible affinity states of a G protein-coupled receptor, whereas for LTC_4, the high affinity site is likely to be a specific LTC_4 receptor.

Cysteinyl-LTs are a family of biologically active compounds derived from arachidonic acid via the 5-lipoxygenase pathway (Murphy *et al*., 1979); they have been shown to be potent bronchoconstrictors (Dahlén *et al*., 1980) in both normal people and asthma patients (Barnes *et al*., 1984). Therefore, the main pathophysiological role of cysteinyl-LTs lies in asthma (Piper *et al*., 1991), which is considered a chronic inflammatory condition characterized not only by bronchial constriction but also by bronchial hyperresponsiveness, mucus hypersecretion, and plasma extravasation. In the latter phenomena, the lung parenchyma plays a fundamental role (Chanarin and Johnston, 1994). For these reasons, an increasing number of studies aimed at the pharmacological characterization of *Cys-LT* receptors have been performed in the respiratory system of different species.

It has been demonstrated that at least two different *Cys-LT* receptors exist in guinea pig airways: one predominantly activated by LTD_4 and LTE_4, and a second predominantly activated by LTC_4. The former is sensitive to the so-called classic antagonists, the most studied of which are SKF 104353, MK 571, ICI 198,615, and Ro 24–5913 (Salmon and Garland, 1991), and has been named *Cys-LT*$_1$, whereas the latter, *Cys-LT*$_2$, is insensitive to the same antagonists (Coleman *et al*., 1995). The nature of *Cys-LT* receptors in human airways has been a matter of debate; it is widely accepted that LTC_4 binds to a variety of nonreceptor sites (i.e., enzymes involved in its synthesis and metabolism and transporters) (Keppler, 1992; Nicholson *et al*., 1992; Metters *et al*., 1994). So far, such binding proteins have impaired the identification of its specific receptor by ligand-binding studies.

The aim of the current study was to characterize the nature and number of cysteinyl-LT binding sites in HLPM. In fact, it has already been demonstrated in this tissue that under controlled metabolic conditions, both LTC_4 and LTD_4 are able to contract isolated human lung strips (Gardiner and Cuthbert, 1988). We used a variety of experimental protocols for ligand binding studies in addition to computer modeling of binding data and GTPase activation. We report the identification of two distinct high affinity binding sites for LTC_4 and LTD_4 that bear the characteristics of specific receptors.

This work was supported in part by Italian National Research Council (CNR) Grants 91.00439.CT04, 92.00719.CT04, and 93.00359.CT04 (S.N.).

ABBREVIATIONS: LT, leukotriene; *Cys-LT*, cysteinyl-leukotriene receptor; *S*-decyl-GSH, (*S*)-decyl-glutathione; HLPM, human lung parenchyma membranes; Gpp(NH)p, guanosine-5′-(β,γ-imido)triphosphate; HPLC, high performance liquid chromatography.

Experimental Procedures

Materials

[^{3}H]LTC_4 (127–173 Ci/mmol) and [^{3}H]LTD_4 (127–173 Ci/mmol) were purchased from DuPont-New England Nuclear (Boston, MA). [γ-^{32}P]GTP (>5000 Ci/mmol) was purchased from Amersham International (Little Chalfont, Buckinghamshire, UK). LTC_4, LTD_4, and LTE_4 were obtained from Cayman Chemical (Ann Arbor, MI). SKF 104353 was kindly provided by SmithKline and Beecham (King of Prussia, PA). ICI 198,615 was kindly provided by Zeneca (Basiglio, Italy). Gpp(NH)p, *S*-decyl-GSH, cysteine, glycine, boric acid, serine, HEPES, and the reagents used for GTPase assay were purchased from Sigma Chemical (St. Louis, MO). Filtercount and Ultima Gold were from Packard Instruments (Meriden, CT). All the reagents used in HPLC analysis were of analytical grade and purchased from Carlo Erba (Milan, Italy), as were GF/C Whatman fiber-glass filters.

Preparation of Human Lung Membranes

Crude membranes were prepared from macroscopically normal human lung specimens that had removed during thoracotomy for lung cancer as described previously (Rovati *et al*., 1985). Briefly, specimens were minced and homogenized at 4° in 10 mM HEPES buffer, pH 7.4 (1:24, w/v), with a Polytron homogenizer (Brinkmann Instruments, Westbury, NY). The homogenate was centrifuged at $770 \times g$ for 10 min, and the supernatant was centrifuged at $27{,}000 \times g$ for 20 min. The pellet was resuspended in the same buffer, centrifuged under the same condition and resuspended in 1/20th of the homogenization volume. The membrane aliquots were frozen at −80° and stored for no longer than 3 months. Protein content was determined with the Bradford dye-binding protein assay (Pierce, Rockford, IL). Before use, serine/borate complex (40 mM), prepared as an equimolar solution of serine and boric acid, cysteine (10 mM), and glycine (10 mM) were added to the membrane suspension to avoid cysteinyl-LT metabolism.

Reversed-Phase HPLC

Before use, labeled and unlabeled leukotriene purity always was assessed by reversed-phase HPLC. Only leukotrienes with a purity grade ≥90% were used. The Beckman Instruments (Columbia, MD) HPLC system was equipped with a 110B Solvent Delivery Module, ODS Ultrasphere C18 column (5 μm, 4.6 mm × 25 cm), and a Programmable Detector Module 166 set at 280 nm. Both labeled and unlabeled leukotrienes were eluted isocratically with a filtered and degassed mixture of $CH_3OH/H_2O/CH_3COOH$ (65:35:0.02), adjusted at pH 5.8 with NH_4OH, at a flow rate of 1 ml/min. To check the purity of tritiated leukotrienes, fractions were collected every 30 sec, and the radioactivity profile was assessed by liquid scintillation counting (Ultima Gold; Packard, Meriden, CT).

Binding Studies

Equilibrium binding studies were performed at 25° for 30 min with 0.02–0.5 nM [^{3}H]LTC_4 or [^{3}H]LTD_4 and unlabeled homologous and heterologous ligands at the indicated concentrations. Heterologous competition curves were performed with 0.5 nM labeled ligand. HLPM (0.25 mg/sample), 10 mM HEPES-KOH, pH 7.4, 1 mM $CaCl_2$, and 10 μM *S*-decyl-GSH (unless otherwise indicated) were added to the incubation mixture to achieve a final volume of 250 μl. Gpp(NH)p was used at a concentration of 30 μM where indicated. Unbound ligand was separated from bound ligand by rapid vacuum filtration (Brandel Cell Harvester) onto glass-fiber GF/C filters soaked in 2.5% polyvinyl alcohol, and the filters were washed twice with 4 ml of HEPES buffer at 4°. Radioactivity was then measured in a liquid scintillation counter (Filter Count; Packard). Nonspecific binding was 35–50% and 25–30% of the total binding (at 0.5 nM labeled ligand) for LTD_4 and LTC_4, respectively. It was calculated by LIGAND as one of the unknown parameters of the model. Each experiment was performed at least three times in triplicate.

Protocol Optimization and Computer Analysis

The program DESIGN (Rovati *et al*., 1988) was used to optimize the binding protocols by selecting the lowest number of most appropriate concentrations in mixed-type curves (Rovati *et al*., 1991) and multiligand experiments (Rovati *et al*., 1990).

Mixed-type curves. The first three to five concentrations (0.02–0.5 nM) in the curves were obtained using increasing concentrations of labeled ligand (saturation part of the curve), whereas the last three to five concentrations (1 nM to 1 μM) were obtained by adding increasing concentrations of unlabeled ligand to a fixed concentration of labeled ligand (homologous competition part of the curve). By effectively combining both saturation and competition protocols in a single curve, high concentrations of the ligands can be reached without consumption of excessive amounts of labeled ligand (competition part of the curve), yet there will be adequate radioactivity in the lower concentration range (saturation part of the curve). This type of protocol is useful when dealing with labeled ligands with a low specific activity (typically tritiated ligands) that interact with high affinity binding sites (Rovati, 1993).

Multiligand protocols. With this type of protocol, the concentrations of both labeled and unlabeled ligands can be varied simultaneously. By definition, these designs allow the use of any combination of two (or more) ligands in each reaction tube; therefore, a multiligand design potentially includes all possible combinations of concentrations of labeled and unlabeled ligand. This three-dimensional binding "surface" may be regarded either as a family of dose-response curves for ligand 1 in the presence of increasing concentrations of ligand 2 or as a family of dose-response curves for ligand 2 in the presence of increasing concentrations of ligand 1. We performed a series of saturation or mixed curves (e.g., with [^{3}H]LTD_4), each in the presence of a fixed concentration of a second unlabeled compound (LTC_4 or an antagonist). In fact, to study an unlabeled ligand (regardless of its K_i value) with a classic heterologous competition curve, a concentration of the labeled ligand must be used that is lower than its K_d, or the so-called self-displacement by the same labeled ligand occurs, thus preventing interaction of the unlabeled ligand with that site (Rovati, 1993). On the other hand, such a low concentration of labeled ligand might yield an amount of bound radioactivity extremely low. To overcome this limit, we extensively used the multiligand protocols.

Computer analysis. Analysis of binding data was performed using the program LIGAND (Munson and Rodbard, 1980). The computerized analysis of the data through the use of LIGAND has several advantages: it allows (1) analysis of the mixed-type curves and multiligand designs; (2) simultaneous analysis of several experiments, thus pooling information from different curves; (3) testing of different models of increasing complexity (i.e., one-site, two-site, possible cross-reactivity, and so on) and selection of the most appropriate model using the *F* test for the extra sum of square principle (Draper and Smith, 1966); (4) direct calculation of K_d and K_i values without any further approximation; and (5) generation of curves according to the model selected. The final model of leukotriene interaction was chosen among several others of lesser or greater complexity according to this principle. A value of $p < 0.05$ was accepted as indicating statistical significance.

The approach used to define the final model was to perform and analyze first the mixed-type curves for each labeled ligand ([^{3}H]LTC_4 and [^{3}H]LTD_4). Once the model for each single ligand was defined, we performed a series of heterologous curves of unlabeled LTC_4 versus labeled LTD_4 and, vice versa, to define whether there was cross-reactivity between them. Successively, we performed a series of multiligand experiments running mixed curves of [^{3}H]LTC_4 in the absence and presence of fixed concentrations of unlabeled LTD_4, and vice versa. With the combined analysis of the experiments, the final model with interaction was built. Finally, a series of heterologous and multiligand curves with the unlabeled antagonists was run using both [^{3}H]LTD_4 and [^{3}H]LTC_4 as labeled ligands; each time, an

optimized homologous curve was included in the same experiment to take into account the variability observed with human tissues.

Binding is expressed as the ratio of bound ligand concentration to total ligand concentration (B/T, dimensionless) versus the logarithm of total ligand concentration (log T). B (in M) is the sum of labeled, nonlabeled, and nonspecific binding; T (in M) is the sum of labeled and nonlabeled ligand incubated. This graphic representation was chosen because it is the only way to present mixed curves (which cannot be presented in the classic form of percentage specific binding) and it allows a direct comparison of mixed, multiligand, and competition curves. All the curves shown were computer generated.

GTPase Activity

The following standard conditions were used to measure the release of $^{32}P_i$ from [γ-^{32}P]GTP on the basis of the method of Cassel and Selinger (1976). The assay system contained 1 μM [γ-^{32}P]GTP (5 Ci/mmol), 2 mM $MgCl_2$, 1 mM 5′-adenylylimidophosphate, 0.5 mM ATP, 10 mM creatine phosphate, 10 mM creatine phosphokinase, 1 mM dithiothreitol, 0.1 mM EDTA, 0.5 mM ouabain, 150 mM NaCl, and 10 mM Tris·HCl, pH 7.4, in a final volume of 0.1 ml. Low affinity hydrolysis of [γ-^{32}P]GTP (high K_m GTPase activity) was assessed by incubating parallel tubes in the presence of 50 mM GTP and was subtracted from the total GTPase activity to calculate high affinity GTPase hydrolysis. The reaction was initiated by the addition of HLPM (0.005 mg of protein) to the mixture at 37° and terminated after a 20-min incubation through removal of the tubes to ice for 3 min and the addition of 0.5% (w/v) active charcoal in H_3PO_4, pH 2.2–2.3, giving a total volume of 1 ml. The $^{32}P_i$ formed was separated from the nonhydrolyzed nucleotide-bound phosphate by centrifugation at 11,000 $\times$ *g* for 5 min. Aliquots (0.5 ml) of the supernatant were removed form each tube and added to scintillation liquid (Ultima Gold; Packard) for radioactivity counting.

Results

[^{3}H]LTC$_4$ and [^{3}H]LTD$_4$ binding. [^{3}H]LTC$_4$ and [^{3}H]LTD$_4$ mixed-type curves (see Experimental Procedures) were performed in the absence and presence of 10 μM *S*-decyl-GSH (Fig. 1). In the absence of *S*-decyl-GSH, only one low affinity class of sites was detectable in most of the experiments with [^{3}H]LTC$_4$ (Fig. 1A), whereas in the presence of *S*-decyl-GSH, at least two classes of sites were present: one with high affinity and low capacity and a second with low affinity and high capacity (Table 1). At variance with [^{3}H]LTC$_4$, [^{3}H]LTD$_4$ binding was practically unaffected by the presence of *S*-decyl-GSH (Fig. 1B and Table 1). On the basis of these data, 10 μM *S*-decyl-GSH was included routinely in LTC$_4$ receptor binding assay.

Both [^{3}H]LTC$_4$ and [^{3}H]LTD$_4$ binding curves on HLPM are biphasic and span >2 orders of magnitude (Fig. 2), revealing an interaction with a high and a low affinity class of sites (Table 2). The heterologous competition curves for LTC$_4$ and LTD$_4$ also are shown and appear to be monophasic (Fig. 2) with K_i values in the low affinity range (Table 2).

To investigate whether LTC$_4$ was able to cross-react with the high affinity site labeled by [^{3}H]LTD$_4$ and vice versa, we performed a series of multiligand experiments [i.e., curves of [^{3}H]LTD$_4$ in the absence and presence of fixed concentrations of LTC$_4$ (0.1, 1, and 10 nM) and curves of [^{3}H]LTC$_4$ in the absence and presence of fixed concentrations of LTD$_4$ (0.1, 1, and 10 nM)] [Fig. 3; for the sake of clarity, only the effect of the highest concentration (i.e., 10 nM) of unlabeled ligand is shown]. The K_i values of each LT versus the sites labeled by the other leukotriene were obtained through simultaneous computer analysis of a family of four different curves (control plus the three multiligand curves at the above indicated concentrations) for each labeled ligand (Table 2). Furthermore, for both ligands, we tested the model that assumes cross-reactivity versus the simpler model that rules it out, by means of the *F* test (see Experimental Procedures) and found that the former was significantly better ($p < 0.05$). Thus, taken together, these results indicated that the unlabeled ligand was able to significantly decrease the binding of the labeled LT.

To validate the results, we simulated (MacSIMUL; G. E. Rovati and P. J. Munson) the theoretical model for the simultaneous interaction of two ligands, each with two different binding sites. In particular, we hypothesized the interaction of a ligand, with the binding characteristic of LTD$_4$ (K_{i1} = 7.7 nM, K_{i2} = 46 nM; Table 2), with the high and low affinity binding sites labeled by another ligand with the binding characteristics of [^{3}H]LTC$_4$ (K_{d1} = 0.015 nM, K_{d2} = 105 nM; Table 2). The simulation was conceived with an extended multiligand protocol (see Experimental Procedures), including the control [^{3}H]LTC$_4$ mixed curve, a family of three multiligand [^{3}H]LTC$_4$ curves, each in the presence of a fixed

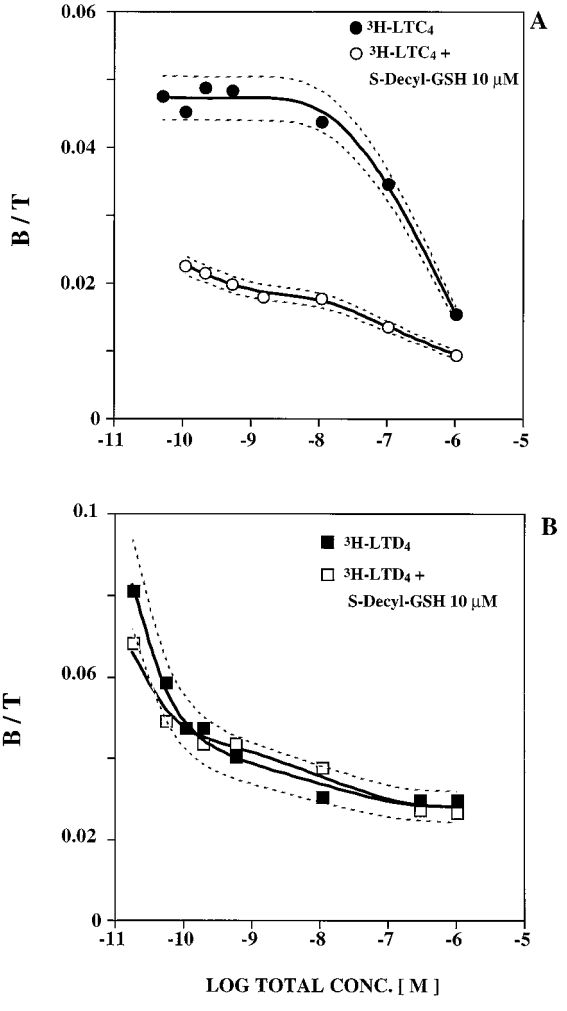

Fig. 1. Effect of *S*-decyl-GSH on [^{3}H]LTC$_4$ and [^{3}H]LTD$_4$ binding. A, Mixed-type curve of [^{3}H]LTC$_4$ in the absence (●) and presence (○) of 10 μM *S*-decyl-GSH. B, Mixed-type curve of [^{3}H]LTD$_4$ in the absence (■) and presence (□) of 10 μM *S*-decyl-GSH. *Dotted lines*, ±95% confidence limits. Data are mean of three replicates from a single experiment, representative of at least two other experiments.

TABLE 1
Effect of *S*-decyl-GSH on ^{3}H-LTC_4 and ^{3}H-LTD_4 binding

Ligand	K_{d1} ± CV%	K_{d2} ± CV%	B_{max1} ± CV%	B_{max2} ± CV%
	nM		*pmol/mg*	
^{3}H-LTC_4		182 ± 19		7.3 ± 22
^{3}H-LTD_4	0.021 ± 61	380 ± 90	0.0016 ± 31	2.67 ± 85
+ 10 μM S-Decyl-GSH				
^{3}H-LTC_4	0.085 ± 50	150 ± 46	0.0033 ± 50	1 ± 49
^{3}H-LTD_4	0.028 ± 33	91 ± 90	0.00083 ± 42	0.47 ± 88

concentration (0.1, 1, and 10 nM) of LTD_4 (Fig. 4). Similar results were obtained in simulation of LTC_4 interaction with [^{3}H]LTD_4 binding sites (results not shown).

Fig. 2 also shows the heterologous curves for LTE_4 using [^{3}H]LTC_4 and [^{3}H]LTD_4 as labeled ligands (Fig. 2, A and B, respectively). Both curves seem to be monophasic revealing the interaction of this leukotriene with the low affinity site labeled by both [^{3}H]LTC_4 and [^{3}H]LTD_4. Moreover, to investigate whether LTE_4 was able to interact with the high affinity sites as well, we performed a series of multiligand experiments (not shown) with both [^{3}H]LTC_4 and [^{3}H]LTD_4 in the absence and presence of fixed concentrations of LTE_4 (0.1, 1, and 10 nM). LTE_4 was able to significantly ($p < 0.01$) displace [^{3}H]LTD_4 from its high affinity sites, whereas it interacted with only the lower affinity site of [^{3}H]LTC_4 (Table 2).

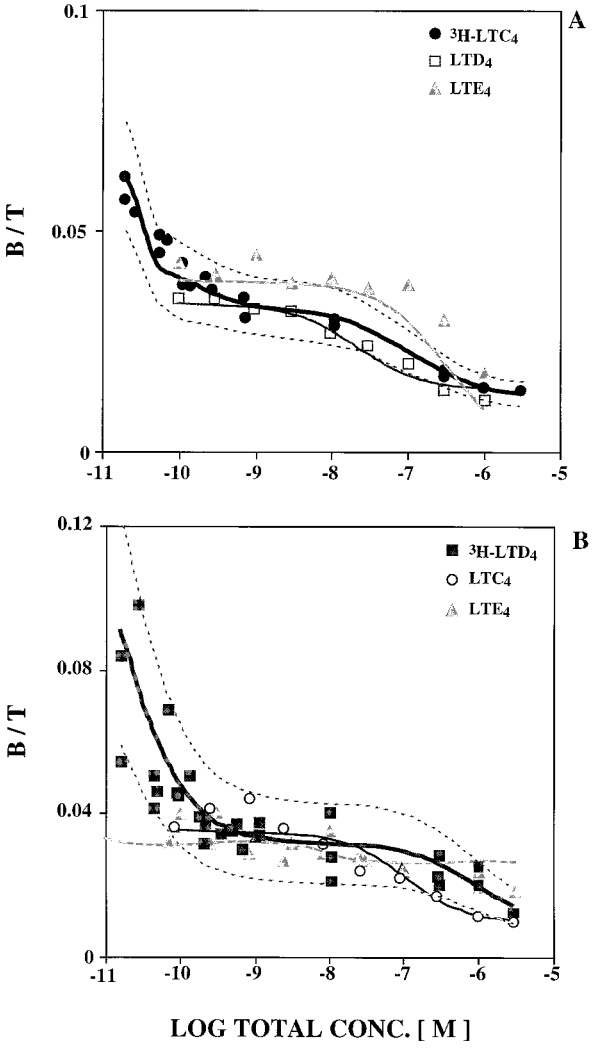

Fig. 2. Homologous and heterologous curves of [^{3}H]LTC_4 and [^{3}H]LTD_4. A, Mixed-type curve of [^{3}H]LTC_4 (●) and heterologous competition curves of LTD_4 (□) and LTE_4 (▲). B, Mixed-type curve of [^{3}H]LTD_4 (■) and heterologous competition curves of LTC_4 (○) and LTE_4 (▲). *Dotted lines*, ±95% confidence limits and are shown only for the control curve, for the sake of clarity. Data are mean of three replicates from one to three different experiments.

We investigated further the nature of LTC_4 and LTD_4 binding to HLPM by studying the effect of Gpp(NH)p, a nonhydrolyzable GTP analog. Fig. 5B shows that 30 μM Gpp(NH)p is able to almost completely shift the high affinity [^{3}H]LTD_4 binding to its low affinity component (Table 3). On the contrary, Gpp(NH)p has only a very small effect on the high affinity site labeled by [^{3}H]LTC_4 (Fig. 5A and Table 3).

Antagonist binding studies. Competition curves were performed with two antagonists of different structural classes, ICI 198,615 (indole derivative) and SKF 104353 (leukotriene analog), using [^{3}H]LTD_4 as labeled ligand (Fig. 6A). The responses, albeit varying in potencies, are monophasic, suggesting an interaction with a homogeneous class of binding sites (Table 4). We also performed multiligand experiments with [^{3}H]LTD_4 in the absence and presence of fixed concentrations of SKF 104353, revealing that this compound is able to interact with both the high and low affinity binding sites labeled by [^{3}H]LTD_4 with the same affinity (Fig. 6B and Table 4).

Fig. 7A shows the competition curves for the same antagonists using [^{3}H]LTC_4 as labeled ligand. ICI 198,615 did not induce any appreciable displacement up to a concentration of 10 μM, whereas the response of SKF 104353 was monophasic (Table 4). Multiligand experiments performed with both compounds revealed that ICI 198,615 was unable to interact with either the high or low affinity sites labeled by [^{3}H]LTC_4 (Fig. 7B and Table 4). On the contrary, SKF 104353 (Fig. 7C) was indeed able to displace [^{3}H]LTC_4 from both the high and low affinity sites (Table 4).

GTPase activity. GTPase activity was assayed in HLPM in response to 100 nM LTC_4 or LTD_4. LTD_4, but not LTC_4,

TABLE 2
Affinities and capacities of the binding sites for cysteinyl-LTs

Unlabeled ligand	^{3}H-LTC_4	^{3}H-LTD_4
LTC_4	K_{d1} = 0.015 ± 82 K_{d2} = 105 ± 23 B_{max1} = 0.0012 ± 33 B_{max2} = 2.6 ± 39	K_{i1} = 7.9 ± 76 K_{i2} = 96 ± 53
LTD_4	K_{i1} = 7.7 ± 88 K_{i2} = 46 ± 22	K_{d1} = 0.023 ± 76 K_{d2} = 230 ± 92 B_{max1} = 0.0019 ± 43 B_{max2} = 4.65 ± 90
LTE_4	K_{i2} = 309 ± 52	K_{i1} = 89 ± 40 K_{i2} = 15 ± 90

K_d and K_i values are expressed in nM. B_{max} values are expressed as pmol/mg of protein. Parameters are expressed as mean ± % coefficient of variation.

was able to significantly ($p < 0.05$) stimulate the receptor-induced hydrolysis of GTP (Fig. 8A). Furthermore, the receptor antagonist SKF 104353 (10 μM) was able to completely inhibit LTD_4-induced stimulation (Fig. 8A), and LTD_4 stimulated the GTPase activity in a dose-dependent manner (Fig. 8B).

Discussion

Despite the efforts by many researchers, no *Cys-LT* receptor has been successfully purified or cloned. This might be due to the fact that these receptors are present in such a scarce amount that even their detection by binding techniques is sometimes difficult. Moreover, it is well known that in cellular membranes, LTC_4 binds predominantly to a number of nonreceptor sites, such as glutathione-*S*-transferase (Metters *et al.*, 1994; Sun *et al.*, 1986), LTC_4 synthase (Nicholson *et al.*, 1992), or transport proteins (Keppler, 1992). Therefore, we used *S*-decyl-GSH, a ligand structurally similar to LTC_4 but devoid of either agonist or antagonist activities (Norman *et al.*, 1987; Sala *et al.*, 1990), to inhibit binding to such nonreceptor sites and thus unmask a putative high affinity LTC_4 receptor. In fact, because LTC_4 is able to contract human isolated lung strips with a potency similar to LTD_4 (Gardiner and Cuthbert, 1988), it is likely that LTC_4, as well as LTD_4, should have a high affinity binding site.

Although only one low affinity/high capacity site was detectable in most experiments in the absence of *S*-decyl-GSH (Fig. 1A), in its presence two sites became detectable. One of them is a previously undetected high affinity site for $[^3H]LTC_4$, with a K_d value in the picomolar range (as the one for $[^3H]LTD_4$), compatible with the hypothesis that this binding protein is a receptor. It is unlikely that this site is one of the enzymes that usually are abundant and for which LTC_4 has a K_d values in the range of tens of nM (Metters *et al.*, 1994), as reported in practically all the previous $[^3H]LTC_4$ binding studies (Pong *et al.*, 1983; Nicosia *et al.*, 1984; Rovati *et al.*, 1985; Civelli *et al.*, 1987; Norman *et al.*, 1987). Indeed, it should be considered that the low affinity binding site for LTC_4 could correspond to the ATP-dependent LTC_4 export pump. This *MRP* gene-encoded protein is strongly expressed in normal lung parenchyma (Narasaki *et al.*, 1996) and has a K_m value of 97 nM (Leier *et al.*, 1994) that is compatible with the K_d value of 105 nM (Table 2) estimated for the low affinity binding site of LTC_4. Moreover, this site has a B_{max} value that is 14% of the value obtained in the absence of *S*-decyl-GSH, indicating that *S*-decyl-GSH is able to inhibit most of the nonreceptor binding. However, we cannot completely rule out the hypothesis that this site might be a mixture of LTD_4 receptors and nonreceptor proteins.

As expected for a ligand with low affinity for enzymes such as glutathione-*S*-transferase (Sun *et al.*, 1986), $[^3H]LTD_4$ binding was basically unaffected by the presence of *S*-decyl-GSH. Indeed, in both the absence and presence of *S*-decyl-GSH, a two-site model was identified without any statistical difference in the K_d and B_{max} values (Fig. 1B and Table 1). Therefore, we can conclude that $[^3H]LTC_4$ and $[^3H]LTD_4$ each recognizes two classes of binding sites.

To investigate whether these sites coincide or are separate entities, a series of heterologous competition curves using LTC_4 and LTD_4 were performed. Both LTC_4 and LTD_4 het-

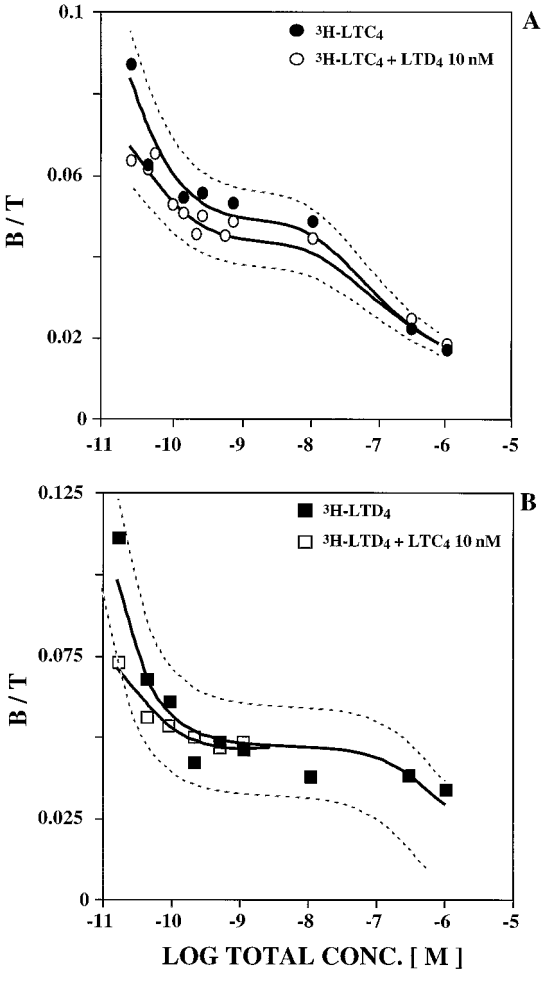

Fig. 3. Multiligand curves of $[^3H]LTC_4$ and $[^3H]LTD_4$. For the sake of clarity, only the effect of the highest concentration of unlabeled ligand (10 nM) is shown. A, Multiligand curve of $[^3H]LTC_4$ in the absence (●) and presence (○) of 10 nM LTD_4. B, Multiligand curve of $[^3H]LTD_4$ in the absence (■) and presence (□) of 10 nM LTC_4. *Dotted lines*, ±95% confidence limits. Data are mean of three replicates from a single experiment, representative of at least two other experiments.

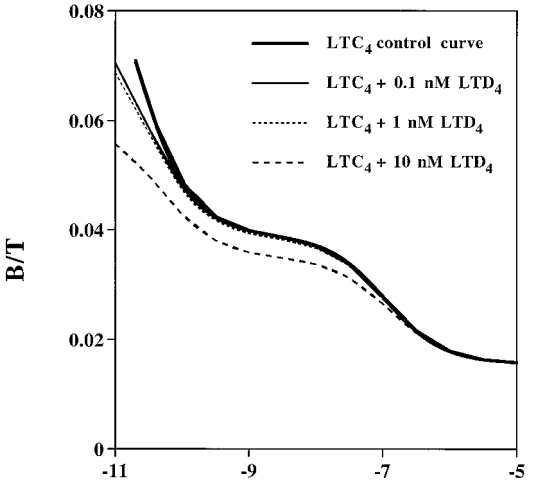

Fig. 4. Theoretical model for the interaction of a ligand, with the binding characteristic of LTD_4 (K_{i1} = 7.7 nM; K_{i2} = 46 nM), with the high and low affinity binding sites labeled by another ligand with the binding characteristics of $[^3H]LTC_4$ (K_{d1} = 0.015 nM; K_{d2} = 105 nM).

erologous competition curves appear to be monophasic (Fig. 2), suggesting that each ligand is able to compete with comparable affinities with the low affinity sites labeled by the other one (Table 2). However, in the case of low specific activity ligands (see Experimental Procedures), this type of experimental protocol does not allow the study of the influence of the nonlabeled heterologous ligand on the high affinity sites labeled by the labeled ligand (Rovati, 1993). Therefore, heterologous competition curve can provide information only on the low affinity site.

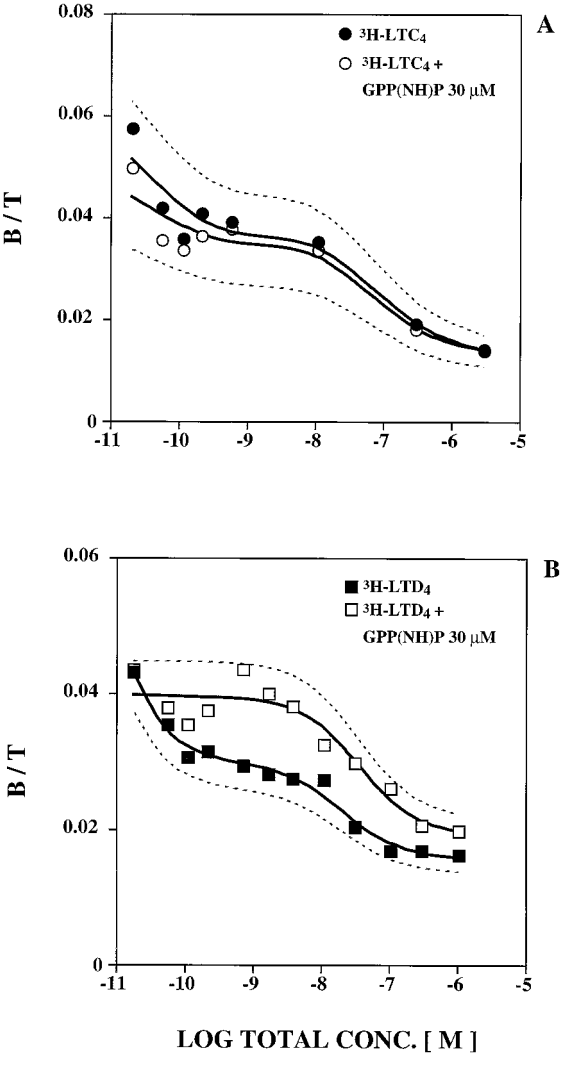

Fig. 5. Effect of Gpp(NH)p on [^{3}H]LTC$_4$ and [^{3}H]LTD$_4$ binding. A, Mixed-type curve of [^{3}H]LTC$_4$ in the absence (●) and presence (○) of 30 μM Gpp(NH)p. B, Mixed-type curve of [^{3}H]LTD$_4$ in the absence (■) and presence (□) of 30 μM Gpp(NH)p. *Dotted lines*, ±95% confidence limits. Data are mean of three replicates from a single experiment, representative of at least two other experiments.

Hence, we applied a multiligand protocol to study the possible influence of LTC$_4$ on the high affinity sites labeled by [^{3}H]LTD$_4$ and vice versa (Fig. 3). Computerized analysis of the data indicated that LTC$_4$ is able to inhibit [^{3}H]LTD$_4$ binding to its high affinity sites and allowed calculation of of a K_i value 520-fold higher than the K$_d$ of [^{3}H]LTC$_4$ for its own high affinity site (Table 2). If LTC$_4$ and LTD$_4$ share the high affinity site, then the K_d and K_i values of LTC$_4$ should have been the same. In the same way, LTD$_4$ is able to inhibit [^{3}H]LTC$_4$ binding to its high affinity sites, with a K_i value 330-fold higher than the K_d of [^{3}H]LTD$_4$ for its own high affinity sites. Interestingly, computer simulation of the proposed model yielded theoretical curves (Fig. 4) that were almost superimposable with the experimental ones (Fig. 3), thus validating the conclusion drawn from analysis of the real data.

These results strongly suggest that the high affinity site labeled by [^{3}H]LTC$_4$ is a different entity from the site labeled by [^{3}H]LTD$_4$ and that there is cross-reactivity between LTD$_4$ and LTC$_4$ high affinity sites. Indeed, it is known from functional studies that in some tissues, so-called classic LTD$_4$ antagonists failed to block the effect of high doses of LTD$_4$ (Gardiner *et al*., 1990). This provides evidence that LTD$_4$ response includes an antagonist resistant component in some tissues (Gardiner *et al*., 1994) that might represent LTD$_4$ interaction with LTC$_4$ receptor.

Heterologous and multiligand curves of LTE$_4$ were also performed using [^{3}H]LTC$_4$ and [^{3}H]LTD$_4$ as labeled ligands. Although LTE$_4$ is able to compete for both LTD$_4$ binding sites, it seems to recognize only the low affinity LTC$_4$ binding site. Moreover, there is ≥1 order of magnitude difference in the K_i values for LTD$_4$ and LTC$_4$ (Table 2); therefore, the LTE$_4$ response also is in agreement with the hypothesis that two distinct receptors exist in HLPM: one more specific for LTD$_4$/LTE$_4$ and one more specific for LTC$_4$.

To investigate the nature of LTC$_4$ and LTD$_4$ putative receptors in HLPM, we studied their potential coupling to a G protein by performing mixed binding curves in the absence and presence of Gpp(NH)p, a stable GTP analog. Gpp(NH)p was able to completely shift [^{3}H]LTD$_4$ binding from the high affinity site to its low affinity site (Fig. 5B), suggesting that these sites represent two interconvertible affinity states of the same receptor and confirming that [^{3}H]LTD$_4$ binds to a G protein-coupled receptor (Mong *et al*., 1986; Crooke *et al*., 1989). On the other hand, the same Gpp(NH)p concentration was not able to substantially affect [^{3}H]LTC$_4$ binding (Fig. 5A). The tiny but reproducible effect of Gpp(NH)p on [^{3}H]LTC$_4$ binding to its high affinity sites might be due to modulation by the GTP analog of the binding of [^{3}H]LTC$_4$ to LTD$_4$ receptor.

To confirm further these data, GTPase activity was assayed in response to both LTC$_4$ and LTD$_4$. LTD$_4$, but not

TABLE 3
Effect of GPP(NH)P on ^{3}H-LTC$_4$ and ^{3}H-LTD$_4$ binding

Ligand	K_{d1} ± CV%	K_{d2} ± CV%	B_{max1} ± CV%	B_{max2} ± CV%
	nM		*pmol/mg*	
^{3}H-LTC$_4$	0.039 ± 40	102 ± 49	0.0012 ± 55	2.5 ± 50
^{3}H-LTD$_4$	0.037 ± 50	22 ± 43	0.0007 ± 22	0.33 ± 42
+ 30 μM GPP(NH)P				
^{3}H-LTC$_4$	0.039 ± 71	86 ± 74	0.0008 ± 50	1.9 ± 77
^{3}H-LTD$_4$		30 ± 40		0.3 ± 42

LTC_4, is able to significantly stimulate GTP hydrolysis over the basal value (Fig. 8A). Furthermore, LTD_4 response is concentration dependent (Fig. 8B), and the receptor antagonist SKF 104353 is able to significantly inhibit LTD_4-induced stimulation of the enzyme (Fig. 8A). Therefore, these data indicate that LTD_4 receptor is indeed coupled to a G protein, whereas the putative specific LTC_4 receptor in HLPM is not coupled to any G protein. A further, but unlikely, hypothesis is that LTC_4 binds to a G protein-coupled receptor (different from that of LTD_4) but behaves as an antagonist, thus being unable to activate GTPase and displaying a GTP-insensitive binding.

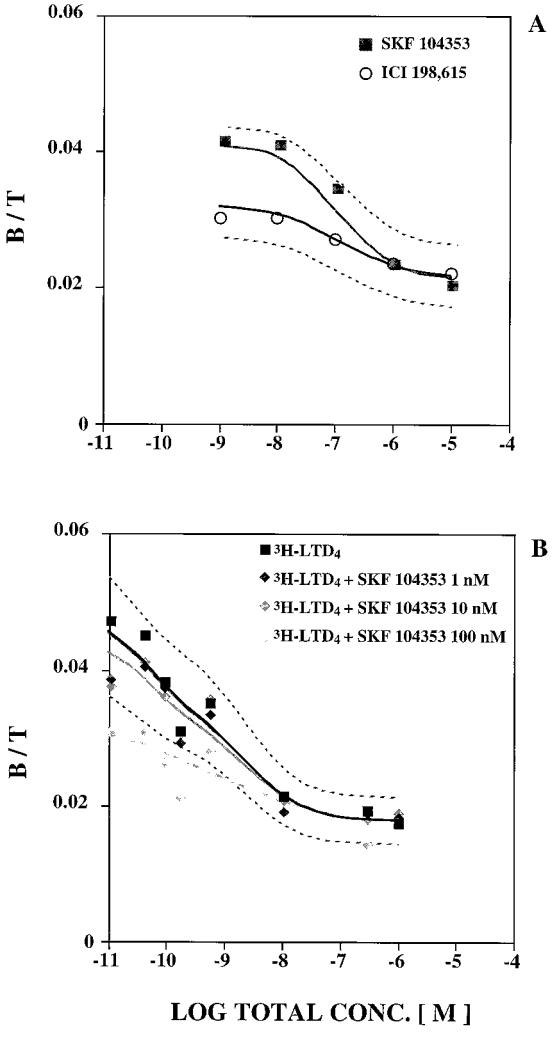

Fig. 6. Antagonist binding curves versus $[^3H]LTD_4$. A, Heterologous competition curves of SKF 104353 (■) and ICI 198,615 (○). B, Multiligand curves of $[^3H]LTD_4$ in the absence (■) and presence (◆) of SKF 104353 at the indicated concentrations. *Dotted lines*, ±95% confidence limits are shown only for the control curve, for the sake of clarity. Data are mean of three replicates from a single experiment, representative of at least two other experiments.

A number of antagonists are available for research, and some are undergoing clinical evaluation. We used two of them to study the pharmacological profile of the putative LTD_4 and LTC_4 receptors. As pure antagonists, they should not distinguish between the high and low affinity state of a G protein-coupled receptor, such as that for LTD_4 (De Lean *et al.*, 1980; Lefkowitz *et al.*, 1993). In fact, the multiligand experiment performed with SKF 104353 (Fig. 6B) confirmed that as expected, this compound interacts with both the high and low affinity states of the LTD_4 receptor with the same affinity. Furthermore, the dissociation constant computed only from the competition curve (Fig. 6A) and the one computed from the multiligand curves are substantially identical (Table 4), making multiligand experiments unnecessary in the case of pure antagonists.

When tested versus $[^3H]LTC_4$ with the classic competition curves (Fig. 7A), only SKF 104353 (not ICI 198,615) has a K_i value lower than 10 μM (Table 4), the value we consider the upper limit for a biologically relevant interaction. For the reasons we discussed, we used a multiligand protocol to study the possible influence of the antagonists on the high affinity sites labeled by $[^3H]LTC_4$ (Fig. 7, B and C). This experiment allowed us to reveal that SKF 104353 is able to compete with both the sites labeled by $[^3H]LTC_4$ with markedly different affinities. Moreover, the affinity for the low affinity site computed from the multiligand experiment is not significantly different from that calculated from the pure competition curve (Table 4). On the contrary, ICI 198,615 is unable to compete with either of the sites labeled by $[^3H]LTC_4$ (Fig. 7B). It is clear from Figs. 6 and 7 that there is a striking difference in the behavior of such antagonists versus $[^3H]LTD_4$ or $[^3H]LTC_4$, again supporting the idea that two different receptors might exist in HLPM.

Taken together, these data indicate that in human lung parenchyma (Fig. 9), (1) $[^3H]LTD_4$ and $[^3H]LTC_4$ recognize two different binding sites, a high affinity one (R_{1H} and R_{2H}) and a low affinity one (R_{1L} and S_{2L}); (2) the two high affinity binding sites are different entities, albeit there is cross-reactivity between LTD_4 and LTC_4; (3) for $[^3H]LTD_4$, the two binding sites represent the interconvertible high and low affinity states of a G protein-coupled receptor; (4) for $[^3H]LTC_4$, the low affinity binding site probably consists of a mixture of proteins, including the low affinity state of the LTD_4 receptor (R_{1L}), specific enzymes, and transport systems (S_{2L}). The high affinity binding site (R_{2H}) might be a specific LTC_4 receptor. Indeed, as mentioned, functional data indicate the existence of a receptor for LTC_4 in human lung

TABLE 4
Affinities of different antagonists for the sites labeled by ^3H-LTD_4 and ^3H-LTC_4

Type of experiment	Antagonist	^3H-LTC_4		^3H-LTD_4	
		K_{i1} ± CV%	K_{i2} ± CV%	K_{i1} ± CV%	K_{i2} ± CV%
			nM		
Competition	SKF 104353	N.D.	2100 ± 16	N.D.	72 ± 92
	ICI 198,615	N.D.	>10,000	N.D.	58 ± 61
Multiligand	SKF 104353	1.5 ± 87	3870 ± 45	75 ± 82	75 ± 82
	ICI 198,615	>10,000	>10,000		

N.D., not detectable.

parenchyma (Gardiner and Cuthbert, 1988), to which a high affinity binding site must correspond.

In conclusion, the characterization of the *Cys-LT* receptors in human lung parenchyma, which is important in the pathogenesis of asthma, may foster the identification of a novel cysteinyl-LT antagonist with an ideal pharmacological profile to be used in the therapy of this chronic disease. The existence of a specific receptor for LTC_4 in this tissue implies that an ideal antagonist should be able to recognize and antagonize not only the LTD_4 receptor but also that specific for LTC_4. In fact, all the antagonists developed up to now, including the dual antagonist BAY u9773, are unable to completely reverse the effect of high doses of LTD_4 or LTC_4 in some tissues (Gardiner *et al.*, 1994), such as human lung, thus limiting the therapeutical efficacy of this class of drugs.

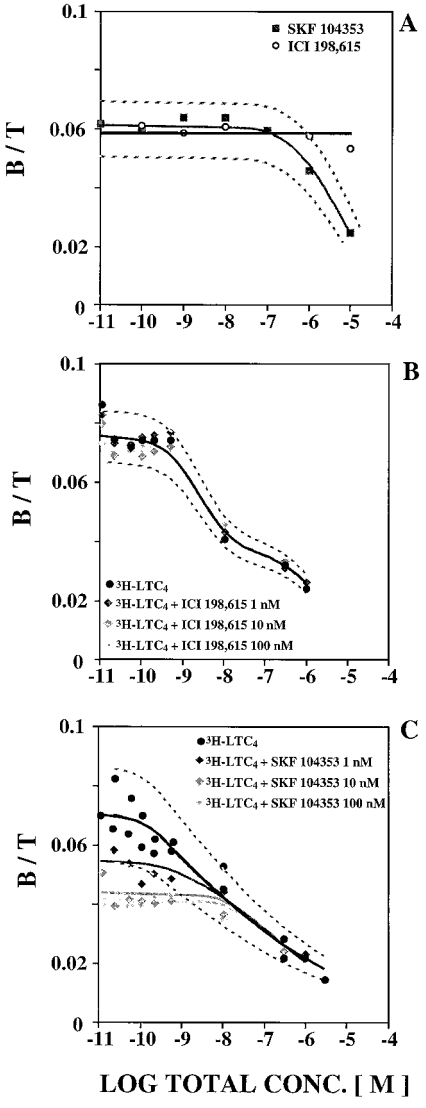

Fig. 7. Antagonist binding curves versus [^{3}H]LTC_4. A, Heterologous competition curves of SKF 104353 (■) and ICI 198,615 (○). B and C, Multiligand curves of [^{3}H]LTC_4 in the absence (●) and presence (♦) of either ICI 198,615 (B) or SKF 104353 (C) at the indicated concentrations. *Dotted lines*, ±95% confidence limits and are shown only for the control curve, for the sake of clarity. Data are mean of three replicates from a single experiment, representative of at least two other experiments.

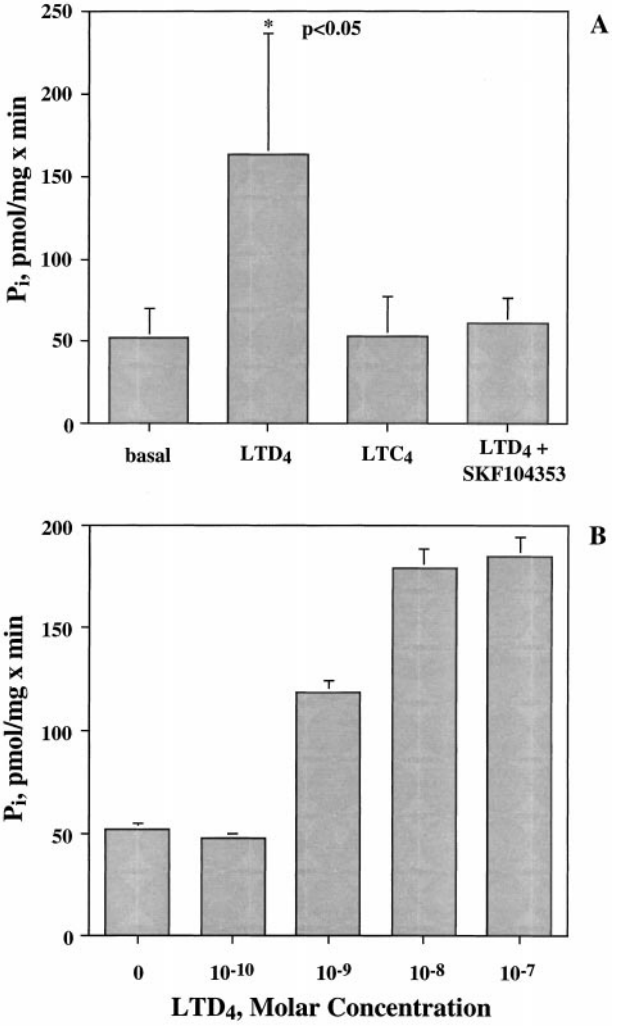

Fig. 8. Effect of LTD_4 and LTC_4 on GTPase activity in human lung parenchyma membranes. A, Effect of 0.1 μM LTD_4, 0.1 μM LTC_4, and 10 μM SKF 104353 plus 0.1 μM LTD_4. B, Dose-response curve for LTD_4. Data are expressed as mean ± standard deviation of seven replicates from a single experiment, representative of at least two other experiments. *, $p < 0.05$ versus basal GTPase activity (one-way analysis of variance).

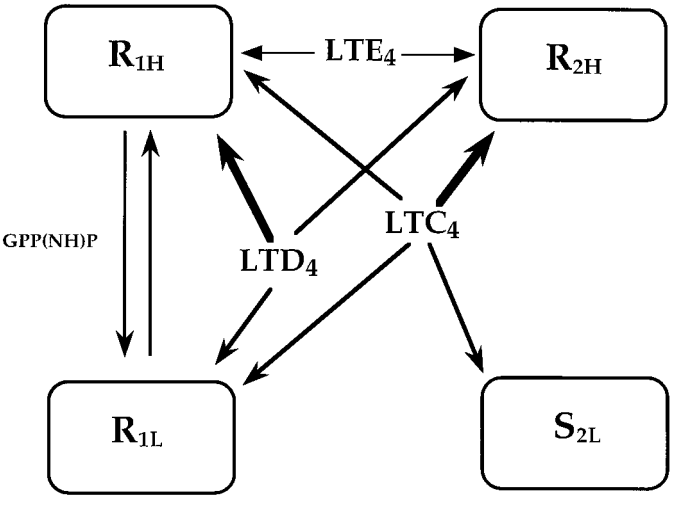

Fig. 9. Final model for *Cys-LT* receptors in human lung parenchyma.

Acknowledgments

We acknowledge the skillful assistance of Dr. M. R. Accomazzo in HPLC analysis of labeled and unlabeled leukotrienes. We are also extremely grateful to Zeneca (Basiglio, Italy) for providing ICI 198,615 and to Drs. M. A. Lewis and H. Sarau (SmithKline Beecham, King of Prussia, PA) for providing SKF 104353.

References

Barnes NC, Piper PJ, and Costello JF (1984) Comparative effects of inhaled leukotriene C_4, leukotriene D_4, and histamine in normal human subjects. *Thorax* **39:**500–504.

Cassel D and Selinger Z (1976) Catecholamine-stimulated GTPase activity in turkey erythrocyte membranes. *Biochim Biophys Acta* **452:**538–551.

Chanarin N and Johnston SL (1994) Leukotrienes as a target in asthma therapy. *Drugs* **47:**12–24.

Civelli M, Oliva D, Mezzetti M, and Nicosia S (1987) Characteristics and distribution of specific binding sites for leukotriene C_4 in human bronchi. *J Pharmacol Exp Ther* **242:**1019–1024.

Coleman RA, Eglen RM, Jones RL, Narumiya S, Shimizu T, Smith WL, Dahlén SE, Drazen JM, Gardiner PJ, Jackson WT, Jones TR, Krell RD, and Nicosia S (1995) Prostanoid and leukotriene receptors: a progress report from the IUPHAR Working Parties on Classification and Nomenclature. *Adv Prostaglandin Thromboxane Leukot Res* **23:**283–285.

Crooke ST, Mattern M, Sarau HM, Winkler JD, Balcarek J, Wong A, and Bennett CF (1989) The signal transduction system of the leukotriene D_4 receptor. *Trends Pharmacol Sci* **10:**103–107.

Dahlén SE, Hedqvist P, Hammarström S, and Samuelsson B (1980) Leukotrienes are potent constrictors of human bronchi. *Nature (Lond)* **288:**484–486.

De Lean A, Stadel JM, and Lefkowitz RJ (1980) A ternary complex model explains the agonist-specific binding properties of the adenylate cyclase-coupled β-adrenergic receptor. *J Biol Chem* **255:**7108–7117.

Draper NR and Smith H (1966) *Applied Regression Analysis*. Wiley, New York.

Gardiner PJ, Abram TS, and Cuthbert NJ (1990) Evidence for two leukotriene receptor types in the guinea-pig isolated ileum. *Eur J Pharmacol* **182:**291–299.

Gardiner PJ, Abram TS, Tudhope SR, Cuthbert NJ, Norman P, and Brink C (1994) Leukotriene receptors and their selective antagonists. *Adv Prostaglandin Thromboxane Leukot Res* **22:**49–61.

Gardiner PJ and Cuthbert NJ (1988) Characterisation of the leukotriene receptor(s) on human isolated lung strips. *Agents Actions Suppl* **23:**121–128.

Keppler D (1992) Leukotrienes: Biosynthesis, transport, inactivation, and analysis. *Rev Physiol Biochem Pharmacol* **121:**1–30.

Lefkowitz RJ, Cotecchia S, Samama P, and Costa T (1993) Constitutive activity of receptors coupled to guanine nucleotide regulatory proteins. *Trends Pharmacol Sci* **14:**303–307.

Leier I, Jedlitschky G, Buchholz U, and Keppler D (1994) Characterization of the ATP-dependent leukotriene C_4 export carrier in mastocytoma cells. *Eur J Biochem* **220:**599–606.

Metters KM, Sawyer N, and Nicholson DW (1994) Microsomal glutathione *S*-transferase is the predominant leukotriene C_4 binding site in cellular membranes. *J Biol Chem* **269:**12816–12823.

Mong S, Wu HL, Stadel JM, Clark MA, and Crooke ST (1986) Solubilization of [^{3}H]leukotriene D_4 receptor complex from guinea pig lung membranes. *Mol Pharmacol* **29:**235–243.

Munson PJ and Rodbard D (1980) LIGAND: a versatile computerized approach for characterization of ligand-binding systems. *Anal Biochem* **107:**220–239.

Murphy RC, Hammarström S, and Samuelsson B (1979) Leukotriene C: slow-reacting substance from murine mastocytoma cells. *Proc Natl Acad Sci USA* **76:**4275–4279.

Narasaki F, Matsuo I, Ikuno N, Fukuda M, Soda H, and Oka M (1996) Multidrug resistance-associated protein (MRP) gene expression in human lung cancer. *Anticancer Res* **16:**2079–82.

Nicholson DW, Ali A, Klemba MW, Munday NA, Zamboni RJ, and Ford-Hutchinson AW (1992) Human leukotriene C_4 synthase expression in dimethyl sulfoxide-differentiated U937 cells. *J Biol Chem* **267:**17849–17857.

Nicosia S, Crowley HJ, Oliva D, and Welton AF (1984) Binding sites for ^{3}H-LTC_4 in membranes from guinea pig ileal longitudinal muscle. *Prostaglandins* **27:**483–494.

Norman P, Abram TS, Kluender HC, Gardiner PJ, and Cuthbert NJ (1987) The binding of [^{3}H]leukotriene C_4 to guinea-pig lung membranes: the lack of correlation of LTC_4 functional activity with binding affinity. *Eur J Pharmacol* **143:**323–334.

Piper PJ, Conroy DM, Costello JF, Evans JM, Green CP, Price JF, Sampson AP, and Spencer DA (1991) Leukotrienes and inflammatory lung disease. *Ann N Y Acad Sci* **629:**112–119.

Pong SS, DeHaven RN, Kuehl FAJ, and Egan RW (1983) Leukotriene C_4 binding to rat lung membranes. *J Biol Chem* **258:**9616–9619.

Rovati GE (1993) Rational design and analysis for ligand binding studies: tricks, tips and pitfalls. *Pharmacol Res* **28:**277–299.

Rovati GE, Oliva D, Sautebin L, Folco GC, Welton AF, and Nicosia S (1985) Identification of specific binding sites for leukotriene C_4 in membranes from human lung. *Biochem Pharmacol* **34:**2831–2837.

Rovati GE, Rabin D, and Munson PJ (1991) Analysis, design and optimization of ligand binding experiments, in *Horizon in Endocrinology. Vol II* (Maggi M and Geenen EV, eds) pp 155–167, Serono Symposia Publication, Raven Press, New York.

Rovati GE, Rodbard D, and Munson PJ (1988) DESIGN: Computerized optimization of experimental design for estimating K_d and B_{max} in ligand binding experiments. I. Homologous and heterologous binding to one or two classes of sites. *Anal Biochem* **174:**636–649.

Rovati GE, Rodbard D, and Munson PJ (1990) DESIGN: Computerized optimization of experimental design for estimating K_d and B_{max} in ligand binding experiments. II. Simultaneous analysis of homologous and heterologous competition curves and analysis of blocking and of 'multiligand' dose-response surfaces. *Anal Biochem* **184:**172–183.

Sala A, Civelli M, Oliva D, Spur B, Crea AEG, Folco GC, and Nicosia S (1990) Contractile and binding activities of structural analogues of LTC_4 in the longitudinal muscle of guinea-pig ileum. *Eicosanoids* **3:**105–110.

Salmon JA and Garland LG (1991) Leukotriene antagonists and inhibitors of leukotriene biosynthesis as potential therapeutic agents. *Prog Drug Res* **37:**9–90.

Sun FF, Chau LY, Spur B, Corey EJ, Lewis RA, and Austen KF (1986) Identification of a high affinity leukotriene C_4-binding protein in rat liver cytosol as glutathione-*S*-transferase. *J Biol Chem* **261:**8540–8546.

Send reprint requests to: Dr. S. Nicosia, Institute of Pharmacological Sciences, University of Milan, Via Balzaretti 9, 20133 Milan, Italy.